Study of the WAAM-CMT process for ER70S steel: Influence of the main parameters on the morphology of single tracks

Eleonora Viola[1,a], Alessia Teresa Silvestri[1,b], Andrea El Hassanin[1,c*] and Antonino Squillace[1,d]

[1]Dept. of Chemical, Materials and Industrial Production Engineering, University of Naples Federico II, Piazzale Vincenzo Tecchio 80, 80125, Naples, Italy

[a]eleo.viola@studenti.unina.it, [b]alessiateresa.silvestri@unina.it, [c]andrea.elhassanin@unina.it, [d]squillac@unina.it

Keywords: Wire Arc Additive Manufacturing, Cold Metal Transfer, Dimensional Accuracy, Statistical Analysis

Abstract. Wire Arc Additive Manufacturing (WAAM) is an emerging technology that enables the production of high-integrity, semifinished metallic components using both conventional and ad-hoc welding machines. However, such a technology presents some challenges, mainly related to obtaining optimal deposition parameters. This experimental study investigated the impact of wire feed speed (WFS) and travel speed (TS) on the geometric properties of WAAM-CMT deposited ER70S single-tracks. The bead width (W) and height (H) were analyzed as response variables. Experimental results revealed that increasing WFS significantly increased both W and H, while increasing TS reduced them. Statistical analysis confirmed the significance of both WFS and TS for W, while only WFS significantly influenced H. These findings highlight the critical role of process parameters in optimizing WAAM geometry, paving the way for enhanced quality in additively manufactured components.

Introduction

Additive Manufacturing (AM) has become a high-demand process due to its ability to improve functionality, productivity, and competitiveness. The leading sectors include automotive, aerospace, medical, and dental industries, as highlighted by Vafadar et al. [1]. The layer-by-layer manufacturing principle minimizes material waste by using only the required amount of material for parts and support structures and enables topological optimization [2]. Furthermore, AM processes make it possible to create hybrid or graded parts by varying material or alloy compositions and to develop tailored structures with optimized properties [3].

This study focuses on a Directed Energy Deposition (DED) technology known as Wire and Arc Additive Manufacturing (WAAM), which employs metallic wire as feedstock and an electric arc as the energy source to melt and deposit material along pre-programmed paths derived from slicing a 3D model. Among metal AM technologies, WAAM stands out as the most advantageous technique for producing components with large dimensions, thanks to its high deposition rate and the virtually unlimited building volume.

To generate the electric arc, different welding techniques can be adopted, including Gas Metal Arc Welding (GMAW), Gas Tungsten Arc Welding (GTAW), and Plasma Arc Welding (PAW). GMAW-based WAAM achieves the highest deposition rates [4]. In the present study a GMAW variant, namely Cold Metal Transfer (CMT), has been investigated. In CMT the wire retraction mechanism decreases the heat input and molten metal transfers in a short-circuit mode to reduce the molten pool size and cooling rate, with nearly spatter free. The reduced heat input offers additional benefits in comparison with GMAW [5,6]. According to Nagasai et al., CMT produces finer microstructure and results in improved mechanical properties of the component [7,8].

However, WAAM has notable drawbacks. As listed by Jafari et al. [9], some common issues are: (i) residual stresses and heat-induced distortions; (ii) poor dimensional accuracy and feature resolution of the component, and (iii) poor surface finish of the manufactured parts. In relation to these aspects, the deposition physics and parameters setting still require further investigation.

WAAM processes employs commercially available wires in spooled form, originally produced for the welding industry. The technology is compatible with different types of metals, including aluminum alloys, titanium alloys, nickel-base superalloys [10], stainless steel [11], low-carbon steel. To date, studies on WAAM-built low-carbon steel parts are still limited.

Recent research has explored how deposition strategies and heat inputs influence microstructure and mechanical properties. For example, Aldalur et al. [12] found that overlapping deposition strategies produced walls with higher hardness, tensile strength, and yield strength compared to oscillatory strategies, due to the finer and heterogeneous microstructure. Le et al. [13] reported that bidirectional deposition strategy produced thin-walls with more consistent height compared to unidirectional strategy. They also found that heat input strongly influenced shape stability but had minimal effect on microstructure type.

Another critical area is the prediction of single-track geometry and optimization of input parameters in WAAM for low-carbon steel. Accurate weld bead dimensions are required, as layer height determines the slicing of the 3D model, and bead width dictates the final component's thickness [14]. Relationships between process parameters and bead geometry are nonlinear and have been modeled using various approaches such as factorial design, regression analysis, artificial neural networks, and response surface methodology.

This study investigates the influence of WAAM process parameters on single-track morphology, using ER70S material in the CMT process, in order to control the final shape of the deposited beads as a function of the desired output.

Materials and methods

In this study, a 1.0 mm diameter mild steel wire (ER70S-6) was used to create 140 mm single tracks for geometric analysis. The average chemical composition of ER70S-6 is shown in Table 1. Mild steel plates were employed as substrates and were securely fixed onto the WAAM machine. The experiments were conducted by varying the wire feed speed (WFS) and travel speed (TS) to examine the influence of these input variables on weld bead profiles. A full factorial design of experiments was implemented, with three levels chosen for each factor, as shown in Table 2. The selection of the values was made with the aim of ensuring a wide process window, within which the variability between different experiments could be observed and captured, also allowing for the identification of potential critical points in the process. Each experiment was repeated three times to evaluate variability within the same test and the stability of the process. Our analysis focused on two key responses to these processing parameters: weld bead height (H) and width (W).

The WAAM system used for the depositions included a Fronius® TransPuls Synergic 4000 CMT source and a Delta Wasp 4070 Industrial 3D printer, as shown in Fig. 1. The built-in Synergic technology enabled the automatic adjustment of welding current (I) and voltage (V) based on WFS and other parameters. In fact, as the feed rate increases, more wire is fed into the weld pool, requiring a higher current to melt the additional wire at the same rate. Consequently, the voltage must be adjusted to maintain a stable arc length and prevent issues like spatter or instability. The set of process parameters used for each experiment is shown in Table 3. The heat input was calculated using the following equation (Eq. 1), where η is set to 0.8 for the CMT process [15]:

$$HI = \frac{\eta \cdot V \cdot I}{TS}, \quad (1)$$

A shielding gas mixture of Ar+2% CO2 was employed at a flow rate of 13 l/min, and the initial contact tip-to-work distance (CTWD) was set to 10 mm for all samples.

Table 1 – Average chemical composition of ER70S-6 wire.

C%	Si%	Mn%	P%	S%	Cu%	Cr%	Ni%	Mo%	Al%	V%	Zr+Ti%
0.070	0.85	1.45	<0.020	<0.020	<0.25	<0.15	<0.15	<0.050	<0.020	<0.030	<0.15

Table 2 – Parameters and their levels.

	Level 1	Level 2	Level 3
WFS [m/min]	2.0	4.5	7.0
TS [mm/s]	4	6	8

Table 3 – Process parameters selected for each experiment.

	WFS [m/min]	TS [mm/s]	Current [A]	Voltage [V]	Heat input [J/mm]
I	7.0	6	194	12.8	331.1
II	4.5	6	148	10.8	213.1
III	2.0	6	71	10.4	98.5
IV	2.0	8	69	10.9	75.2
V	7.0	8	194	12.8	248.3
VI	7.0	4	175	19.3	675.5
VII	4.5	4	148	14.0	414.4
VIII	4.5	8	150	13.8	207.0
IX	2.0	4	71	10.4	147.7

For the measurement procedure, a Leica DCM 3D confocal microscope was used. All samples' widths and heights were acquired at three defined measuring points, distanced by 40 mm along the sample length. The mean value was first calculated for each sample and subsequently averaged across the entire experiment.

The data were analyzed using Design-Expert software. Two separate Analyses of Variance were conducted: one for the variable W and one for the variable H. A 95% confidence level was chosen.

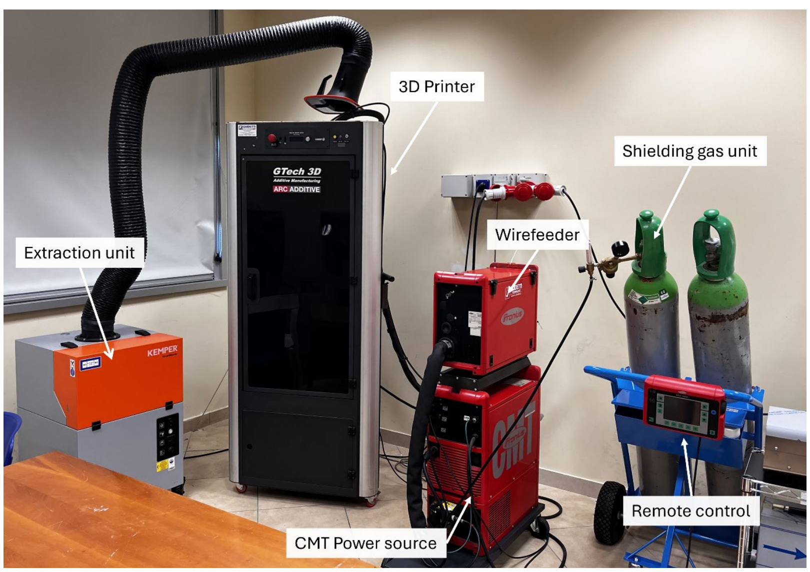

Figure 1 – WAAM-CMT set-up.

Results and discussion

This section explores how the process parameters affected the process stability and the morphology of single tracks, as shown in the first place by the visual aspect of the beads illustrated in Fig. 2.

The first noticeable aspect is that experiments III, IV and IX did not produce continuous single tracks; instead, they resulted in a chain of small spheres. This outcome, consistently observed when the WFS was set to 2 mm/min, is likely due to an insufficient supply of filler material, which prevented the formation of a stable and evenly distributed molten pool. Conversely, the remaining conditions produced continuous beads, whose characteristic dimensions presented a notable variability. The mean values of Width and Height, calculated as described in the previous section, were then used as input data for the statistical analysis.

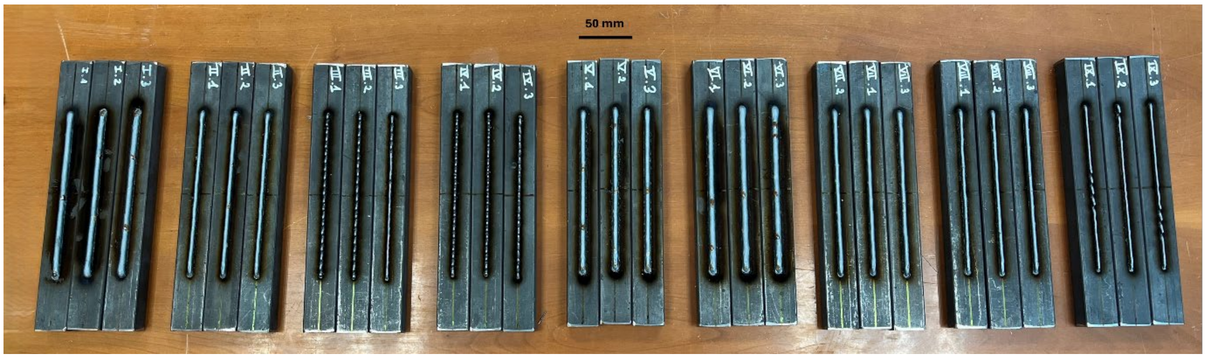

Figure 2 – Single tracks deposited.

Effect of process parameters on width. It is evident that increasing the wire feed speed leads to a significant increase in bead width (W). This phenomenon can be attributed to the higher material deposition rate and the corresponding increase in welding current. As a result, the increased WFS generates larger melt pools, enlarging the weld beads. Conversely, increasing the travel speed reduces the amount of material deposited and the heat input per unit length, resulting in narrower weld beads and a decrease in W. These insights offer valuable guidance for optimizing WAAM processes. For instance, a high value of WFS enhance productivity by increasing the deposition rate. The chosen regression model is linear. The interaction term WFS·TS was not taken into account to avoid multicollinearity, as these two independent variables are highly correlated due to the heat input. Multicollinearity can cause instability in the coefficient estimates. Fig. 3 illustrates Surface Response for width along with the results of the ANOVA. The results highlighted the statistical significance of the model and the process parameters. The Model F-value, combined with a p-value lower than 0.0001, indicates that the overall model is highly significant. Regarding the effect of the independent variables, the p-values confirm that both WFS and TS have a highly significant impact on the dependent variable, although the effect of TS is less pronounced. The determination coefficients demonstrate an excellent fit of the model to the data and the Adequate Precision value underscores the strong signal-to-noise ratio of the model.

The resulting predictive model for W is expressed by the following equation (Eq. 2):

$$W = 2.51667 + 0.566667\, WFS - 0.150000\, TS, \tag{2}$$

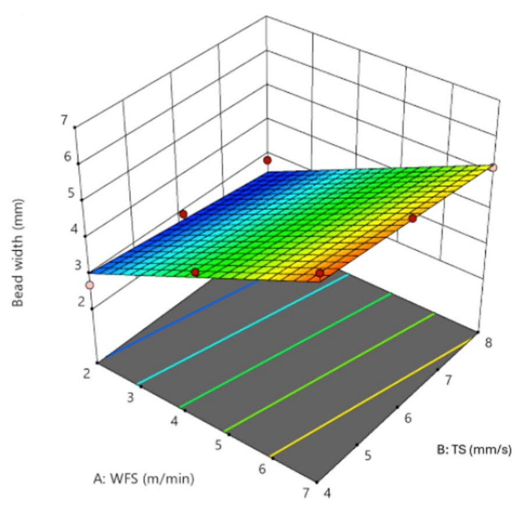

Source	F-value	p-value
Model	86.11	< 0.0001
A-WFS	164.83	< 0.0001
B-TS	7.39	0.0347
R^2		0.9663
Adjusted R^2		0.9551
Predicted R^2		0.9065
Signal-to-noise ratio		22.0014

Figure 3 – Response Surface and ANOVA results for the width of the beads.

Effect of process parameters on height. It was observed that an increase in WFS led to an increase in bead height (H), whereas an increase in TS caused its reduction. This behavior can be explained by the same observations discussed earlier. In this case as well, the linear model proved to be optimal. Fig. 4 shows the Response Surface for height and the ANOVA results, both showing that the overall model is statistically significant. Examining the p-values of the independent variables, it is evident that WFS has a significant effect on the dependent variable, whereas TS does not. This result can be explained by the nature of the welding process. Bead height is determined by the last area to solidify, which may reduce the influence of TS. Indeed, the final stages of solidification occur after the torch has left the area and depend on the accumulated heat and the amount of deposited material, both of which are primarily governed by WFS. At higher TS, the cooling time may be shorter; however, if WFS is sufficiently high, the material may accumulate in greater quantities and solidify into a thicker layer, regardless of travel speed. Conversely, at lower TS, more heat might accumulate in the fusion zone, but if the amount of deposited material is still dictated by WFS, the height may not vary drastically since the bead has time to "self-level" before solidification. It is also important to note that data was collected also from discontinuous single tracks, where it becomes more challenging to obtain accurate and consistent height measurements due to sections with variable heights or localized peaks. This adds noise into the data, reducing the ability to detect a clear effect of TS on bead height. Despite these challenges, the model explains a substantial portion of the variance and demonstrates a strong signal-to-noise ratio.

The resulting predictive model for W is expressed by the following equation (Eq. 3):

$$H = 2.92222 + 0.233333\, WFS - 0.158333\, TS. \quad (3)$$

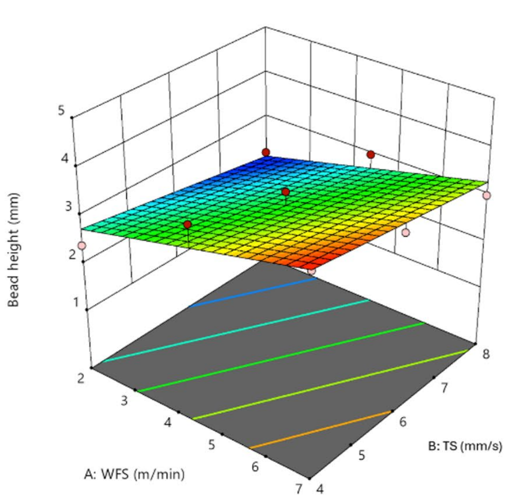

Source	F-value	p-value
Model	11.46	0.0089
A-WFS	17.70	0.0056
B-TS	5.22	0.0625
R^2	0.7925	
Adjusted R^2	0.7233	
Predicted R^2	0.5314	
Signal-to-noise ratio	9.1788	

Figure 4 – Surface Response and ANOVA results for the heigth of the beads.

Conclusions

This study investigated the influence of the main process parameters on the morphology of single tracks in the WAAM-CMT technology applied to ER70S-6 carbon steel. Specifically, the width and height of the weld beads were studied in response to different values of wire feed speed (WFS) and travel speed (TS).

The main objective was to provide guidelines for selecting these parameters to ensure process stability and optimal deposition control for the considered material. For this purpose, an experimental plan was developed with three levels for each of the two factors (WFS and TS), and three repetitions were performed for each combination. Subsequently, an analysis of variance was carried out for each dependent variable (W and H).

The results reveal the following key findings:

- In the range of TS from 4 to 8 mm/s, continuous single tracks cannot be deposited with a WFS of 2 mm/min.
- An increase in WFS leads to an increase in both the width and height of the bead, while an increase in TS causes a reduction.
- Statistical analysis confirmed that both independent variables (WFS and TS) are significant for the model describing the width (W), while only WFS is significant for the model describing the height (H).
- A set of process parameters is established for the deposition of more complex structures, like thin walls and single layers.

The selection of the parameters depends on the objective being pursued. In general, the WAAM-CMT technology is preferred for its high deposition rates. To maximize them, high values of WFS and moderate values TS are preferred. In fact, high TS may require additional passes to complete the component, which reduces the overall process efficiency.

If the goal is to achieve better resolution of the part, lower values for both WFS and TS are recommended. However, it is important to note that excessively low TS leads to the formation of wider beads and increases the risk of thermal distortions.

This study draws the basis for further research, such as the analysis of thin-wall deposition and the creation of complete components, with the aim of gaining a deeper understanding of WAAM-CMT technology.

Furthermore, this methodology has been demonstrated to be effective for the ER70S-6 material and holds potential for studying other materials of industrial interest.

References

[1] A. Vafadar, F. Guzzomi, A. Rassau, and K. Hayward, "Advances in metal additive manufacturing: A review of common processes, industrial applications, and current challenges," 2021. https://doi.org/10.3390/app11031213

[2] J. ZHU, H. ZHOU, C. WANG, L. ZHOU, S. YUAN, and W. ZHANG, "A review of topology optimization for additive manufacturing: Status and challenges," *Chinese Journal of Aeronautics*, vol. 34, no. 1, pp. 91–110, Jan. 2021. https://doi.org/10.1016/J.CJA.2020.09.020

[3] A. T. Silvestri, S. Amirabdollahian, M. Perini, P. Bosetti, and A. Squillace, "Direct laser deposition for tailored structure," *ESAFORM 2021 - 24th International Conference on Material Forming*, 2021. https://doi.org/10.25518/ESAFORM21.4124

[4] B. Wu *et al.*, "A review of the wire arc additive manufacturing of metals: properties, defects and quality improvement," *J Manuf Process*, vol. 35, pp. 127–139, Oct. 2018. https://doi.org/10.1016/J.JMAPRO.2018.08.001

[5] A. El Hassanin, G. Campatelli, R. Sepe, A. T. Silvestri, and A. Squillace, "Effect of energy input on fatigue crack growth behavior of titanium alloy Ti6Al4V made by WAAM-CMT," *Fatigue Fract Eng Mater Struct*, vol. 47, no. 4, pp. 1466–1481, Apr. 2024. https://doi.org/10.1111/FFE.14257

[6] G. H. S. F. L. Carvalho, A. T. Silvestri, G. Campatelli, and A. Squillace, "Effect of cooling strategies on Inconel 625 components produced by wire arc additive manufacturing," *International Journal of Advanced Manufacturing Technology*, vol. 133, no. 7–8, pp. 3631–3646, Aug. 2024. https://doi.org/10.1007/S00170-024-13978-X/TABLES/7

[7] B. P. Nagasai, S. Malarvizhi, and V. Balasubramanian, "Effect of welding processes on mechanical and metallurgical characteristics of carbon steel cylindrical components made by wire arc additive manufacturing (WAAM) technique," *CIRP J Manuf Sci Technol*, vol. 36, pp. 100–116, Jan. 2022. https://doi.org/10.1016/J.CIRPJ.2021.11.005

[8] B. P. Nagasai, S. Malarvizhi, and V. Balasubramanian, "Mechanical properties and microstructural characteristics of wire arc additive manufactured 308 L stainless steel cylindrical components made by gas metal arc and cold metal transfer arc welding processes," *J Mater Process Technol*, vol. 307, p. 117655, Sep. 2022. https://doi.org/10.1016/J.JMATPROTEC.2022.117655

[9] D. Jafari, T. H. J. Vaneker, and I. Gibson, "Wire and arc additive manufacturing: Opportunities and challenges to control the quality and accuracy of manufactured parts," *Mater Des*, vol. 202, 2021. https://doi.org/10.1016/j.matdes.2021.109471

[10] H. Pant, A. Arora, G. S. Gopakumar, U. Chadha, A. Saeidi, and A. E. Patterson, "Applications of wire arc additive manufacturing (WAAM) for aerospace component manufacturing," *International Journal of Advanced Manufacturing Technology*, vol. 127, no. 11–12, pp. 4995–5011, Aug. 2023. https://doi.org/10.1007/S00170-023-11623-7/FIGURES/2

[11] S. K. Sharma and C. Sharma, "Processing Techniques, Microstructural and Mechanical Properties of Wire Arc Additive Manufactured Stainless Steel: A Review," *Journal of The Institution of Engineers (India): Series C*, vol. 103, no. 5, pp. 1325–1339, Oct. 2022. https://doi.org/10.1007/S40032-022-00853-5/FIGURES/13

[12] E. Aldalur, F. Veiga, A. Suárez, J. Bilbao, and A. Lamikiz, "High deposition wire arc additive manufacturing of mild steel: Strategies and heat input effect on microstructure and

mechanical properties," *J Manuf Process*, vol. 58, pp. 615–626, Oct. 2020. https://doi.org/10.1016/J.JMAPRO.2020.08.060

[13] V. T. Le, D. S. Mai, and Q. H. Hoang, "A study on wire and arc additive manufacturing of low-carbon steel components: process stability, microstructural and mechanical properties," *Journal of the Brazilian Society of Mechanical Sciences and Engineering*, vol. 42, no. 9, pp. 1–11, Sep. 2020. https://doi.org/10.1007/S40430-020-02567-0/FIGURES/10

[14] A. T. Silvestri, P. Bosetti, and A. Squillace, "Laser-Directed Energy Deposition of H13: processing window and improved characterization procedures," *Materials and Manufacturing Processes*, vol. 38, no. 14, pp. 1770–1784, Oct. 2023. https://doi.org/10.1080/10426914.2023.2219302

[15] Y. Zhao, F. Chen, S. Cao, C. Chen, and R. Xie, "Effect of CMT Welding Heat Input on Microstructure and Properties of 2A14 Aluminum Alloy Joint," *Metals 2022, Vol. 12, Page 2100*, vol. 12, no. 12, p. 2100, Dec. 2022. https://doi.org/10.3390/MET12122100